

# Transient surface impedance (TranSIM) measurements using discrete lightning for electromagnetic mapping at audio frequencies

**Artyom Emelyanenko\***  
Griffith University  
Nathan, QLD 4111, Australia  
tom.emelyanenko@griffithuni.edu.au

**David V. Thiel**  
Griffith University  
Nathan, QLD 4111, Australia  
d.thiel@griffith.edu.au

\*presenting author

## SUMMARY

The paper describes the first field measurements using recently developed TranSIM instrumentation. The method is based on registering horizontal components of electric and magnetic field of distant lightning strokes (sferics). In fact it is an expansion of classical MT method in the VLF frequency range of 3 to 30 kHz thus providing information about conductivity distribution at the depths of approximately 50 to 300 meters.

Measurements are conducted atop basalt body in the vicinity of Ipswich (Queensland) over 16 sites on 2 parallel profiles. From 20 to 50 sferics were registered at every site. Data was processed using short time Fourier transform obtaining spectrograms of electric and magnetic field. Apparent resistivity was calculated and frequency pseudo sections are presented.

The apparent resistivity sections were matched with geological scheme of the site. Highly resistive zones correlate with high thickness of a basalt layer and conductive zones show where the underlying basalt sandstone is closest to the surface.

**Key words:** impedance method, electromagnetic geophysics, conductivity, sferics.

## INTRODUCTION

Observations of natural electromagnetic field of the Earth have been used during geophysical investigations since the middle of the previous century. There are several sources of this field as, for example, system of currents flowing in ionosphere or lightning strikes occurring worldwide at an average yearly rate of approximately 40 flashes per second (Oliver, 2008). Cagniard (1953) proposed to use magnetotelluric method (MT) utilizing natural time-varying electromagnetic field of the Earth for ground explorations. In the following decades the method went through significant improvement in both data acquisition and processing techniques becoming one of the most useful tools for mining, hydrothermal and structural geophysical explorations.

In 1960s the first attempts were made to utilize field of distant lightning strokes as a source of electromagnetic waves. Jöhler and Lilley (1961) showed that it is possible to use sferic pulses from thunderstorms to determine the conductivity of the ground. Aside from a different source of the electromagnetic waves the main difference of this method from MT sounding is a higher frequency range of observation. In their work Barr, *et al.* (2000) stated that EM field of a lightning strike has dominant part of its spectrum in the frequency range of 500 Hz to 30 kHz which provides information about conductivity distribution for shallower region of the ground compared to MT.

Garner and Thiel (2000) provided further development of the method proposed by Jöhler and Lilley demonstrating that discrete sferics can be used as a source for broad-band (187.5 Hz to 24 kHz) surface impedance measurements (VLF-MT). According to the authors in the presence of strong signal, interpretable impedance information can be obtained from very short sampling intervals (less than 25 s) and possibly even a single discrete sferic. The technique they developed could be useful in number of exploration applications, filling a niche between audio-magnetotelluric and ground penetrating radar.

These investigations followed construction of a VLF sferic probing system – TranSIM (Mogensen *et al.* 2014) which was used in the research.

## MAGNETOTELLURIC METHOD

The main idea of MT method is in registering of horizontal mutually orthogonal components of electric and magnetic field on the Earth's surface and further determination of surface impedance using the equation:

$$Z = \frac{E_x}{H_y} \quad (1)$$

where  $E_x$  is a x component of electric field and  $H_y$  is a y component of magnetic field. This ratio depends on the resistivity of the medium underneath the observation point. The apparent resistivity is a parameter showing resistivity of a uniform half space which would provide the same value of surface impedance and is equal to:

$$\rho = \frac{|Z|^2}{\omega\mu_0} \tag{2}$$

where  $\omega$  is a cyclic frequency and  $\mu_0$  is the magnetic permeability. Thus performing observations on different frequencies or evaluating different parts of frequency spectra it is possible to get information related to resistivity distribution on different depths.

Sferics are seen on a spectrogram as very short wide-frequency bursts. Figure 1 shows several examples of sferics registered by WWLLN (world-wide lightning location network) observatory at Murdoch University, Perth. On the spectrogram it is seen that the biggest amount of energy carried by sferics is contained in the range from approximately 3 to 25 kHz. During data processing in AMT and MT those bursts are usually excluded from the consideration and treated as noise.

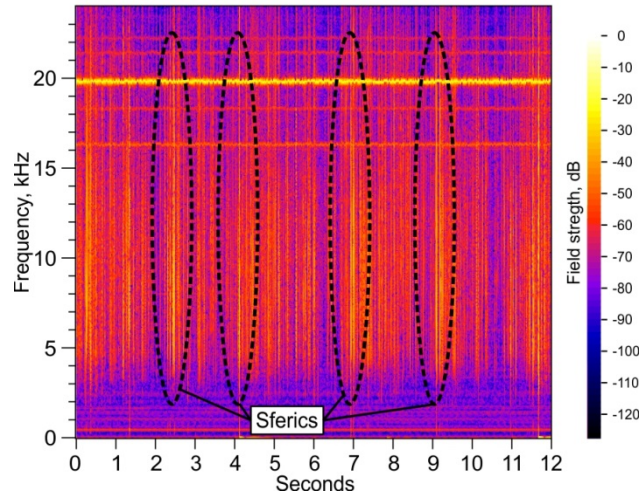


Figure 1: Wideband VLF spectrograms from WWLLN station at Murdoch University, Perth showing sferics. The dashed line ellipses indicate the higher energy sferics.

### DATA REGISTERING AND PROCESSING

TranSIM instrumentation allows registering horizontal orthogonal components of electric and magnetic fields. The sampling frequency is 100 kSamples per second. The magnetic antenna is constructed as multi-coil antenna built around a split core brass former with multiple ferrite rods inserted through the core former. The electric field antenna consists of a simple whip antenna constructed from a single insulated wire conductor. Thiel and Mittra (1997) has demonstrated that the traditional methods of using stacked voltage probes for measurement of electric field could be replaced with an insulated wire dipole to provide an equally reliable measurement technique. Using unstacked wire saves time during field work and makes it easier to conduct one.

Data acquisition was carried out atop effusive tertiary basalt body underlain by weathered Jurassic age sedimentary rocks. The thickness of basalt varies significantly from less than 10 m to more than 138 m. We have the geological model of the test polygon based on 35 boreholes distributed over approximately 0.5 sq km on the site.

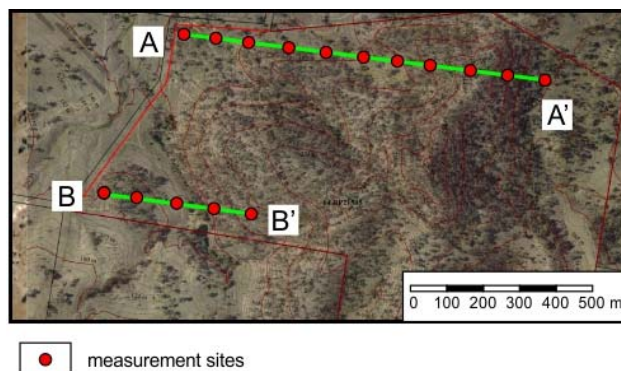


Figure 2 Position of measurement sites. Ipswich vicinity, QLD.

Figure 2 shows positions of the observation sites where measurements were made with TranSIM device. 16 points located on 2 parallel profiles are covered. Approximately 40 sferics were acquired at every measurement site. Figure 3 shows an example of raw

electric and magnetic field signals registered during the observation as well as spectrograms of those signals. Shown spectrograms were calculated using a windowed Fourier transform. Calibrations for sensitivity of magnetic and electric antennas were applied to the spectra.

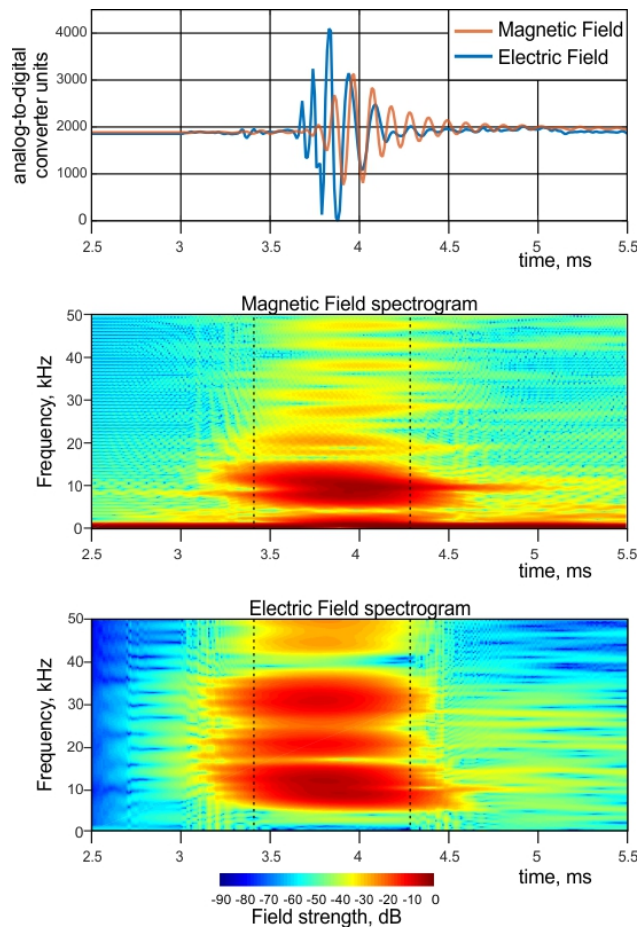


Figure 3 Example of registered sferic and corresponding spectres of magnetic and electric fields. Vertical dotted lines on the spectrogram mark the time band used for further processing.

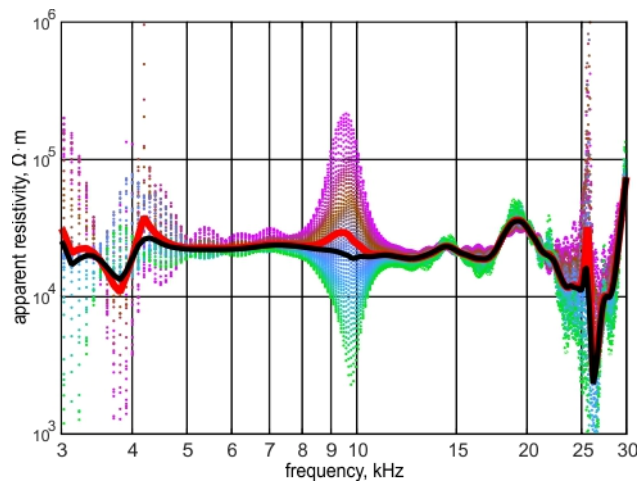


Figure 4 Set of apparent resistivity curves for a single sferic. The colour gradient corresponds to different positions of a window for short time Fourier transform. Thick red and black lines are correspondingly simple average and weighted average curves

As it seen on the graph the duration of the event is less than 1 ms. For assessment of apparent resistivity only those parts of the time series directly containing signal from sferics were used. For every moment of time  $t_i$  inside chosen interval, the apparent resistivity was calculated using (1) and (2). Example of the processing results is shown in the Figure 4.

The number of apparent resistivity estimations for every frequency is equal to the width of time interval used for the processing multiplied by the sampling frequency. The data is consistent within the frequency interval 5 kHz to 20 kHz except for frequency 10 kHz which is resonant frequency of the magnetic coil.

In order to obtain frequency sections averaging of the data at every measurement site for all registered sferics has been made. Weighted average apparent resistivity curve at every frequency  $f_j$  was calculated as:

$$\rho(f_j) = \frac{\sum_{i=0}^N \rho(t_i, f_j) \cdot |H(t_i, f_j)|}{\sum_{i=0}^N |H(t_i, f_j)|} \quad (3)$$

where  $|H|$  is an amplitude of magnetic field spectra and  $N$  is number of apparent resistivity estimations for all sferics on the current site.

The main idea of using amplitude of magnetic field as the weights represents different sferics that have different spectral composition. We place more emphasis on the data obtained from a sferic with bigger amplitude of magnetic field as it provides us with bigger signal to noise ratio.

### COMPARISON WITH A BOREHOLE DATA

The set of apparent resistivity curves obtained during processing was used to build up frequency resistivity sections. Comparison between the sections and geological schemes based on borehole data is presented on the Figure 5 for profile A-A' and on the Figure 6 for profile B-B'. Unfortunately geology schemes were provided for very limited territory. Figure 5 shows highest values of apparent resistivity at profile distances 600-850 meters which coincides with the highest thickness of a basalt layer. As we see from geological scheme, the thickness of the basalt layer declines at profile distances 400 m and 900 m where on the geoelectric pseudo sections we see smaller values of apparent resistivity. Since we expect basalt resistivity to be much higher than that of sandstone, correlation of the highly resistive zones with higher thickness of basalt layer is expected.

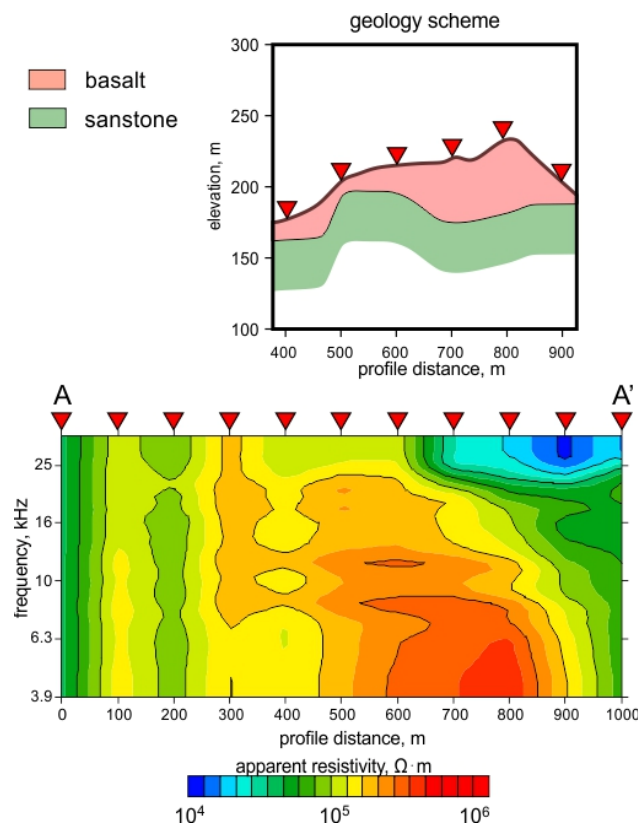
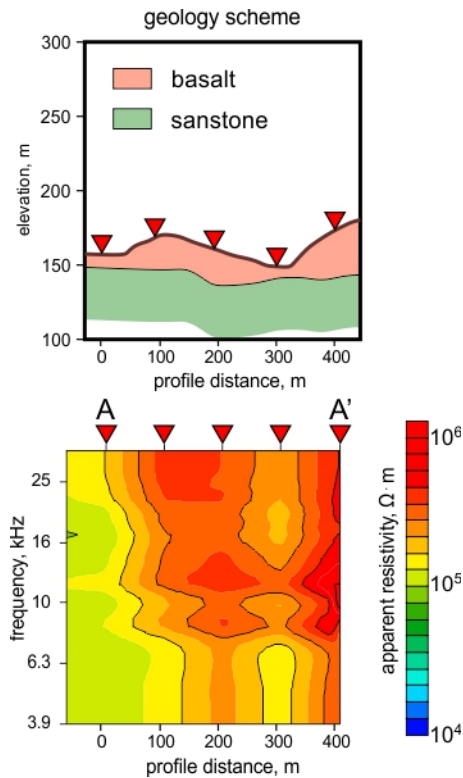


Figure 5 Comparison between apparent resistivity pseudo section and geological scheme for profile A-A'



**Figure 6 Comparison between apparent resistivity pseudo section and geological scheme for profile B-B'**

A similar situation is evident on the profile B-B'. Two highly resistive zones at 100-200 and 350-400 meters are accompanied by the biggest thickness of the basalt layer. The decrease of the thickness is accompanied by the slightly more conductive zones at 0 and 300 metres. The difference between results presented on Figures 5 and 6 is in the frequency position of highly resistive anomalies – for profile A-A' values of apparent resistivity at higher frequencies are lower than those on profile B-B'. It may be explained by a presence of fresh basalt on profile B-B' from the surface while on profile A-A' top layer of basalt is weathered.

## CONCLUSIONS

Data registered during field work with TranSIM instrumentation shows consistency in the range of 3 to 25 kHz providing information about resistivity distribution in the depth range of 50 to 300 meters. The method utilizes naturally occurring electromagnetic field produced by lightning events and consequently does not need an artificial signal transmitter. The whole instrumentation used during field work can be easily carried by a single person. The high rate of natural occurring spheric signal allows reducing measurement time on a site to several minutes.

One of disadvantages of a method is that the sferics producing signal for the registrations should be in the far field that makes it difficult to conduct measurements in the tropic areas near the equator and in the direct proximity (less than 150 km from a thunderstorm).

The matching of the experimental results at testbed site in the vicinity of Ipswich with geological scheme of the site shows correlation of apparent resistivity sections with resistivity distribution in the top 100 meters underneath the surface.

Future scope of work includes parallel simultaneous spheric registration at different sites in order to have a possibility of a data processing with a base station.

## ACKNOWLEDGMENTS

Authors would like to acknowledge Griffith University International Postgraduate Research Scholarship (GUIPRS) scheme and Griffith University Postgraduate Research Scholarship (GUPRS) scheme. The authors also thank Wes Nichols from GeoConsult Pty Ltd for help during field works and useful advices.

## REFERENCES

- Barr, R., D. Llanwyn Jones, and C. J. Rodger, 2000, ELF and VLF radio waves: *Journal of Atmospheric and Solar-Terrestrial Physics*, 62.17, 1689-1718.
- Cagniard, L. 1953, Basic theory of the magneto-telluric method of geophysical prospecting: *Geophysics*, 18(3), 605-635.

Garner, Stephen J., and Thiel, 2000, Broadband (ULF-VLF) surface impedance measurements using MIMDAS, *Exploration Geophysics* 31.1/2, 173-178.

Johler, J. R. and Lilley, C. M., 1961, Ground-conductivity determinations at low radio frequencies by an analysis of the spheric signatures of thunderstorms: *Journal of Geophysical Research*, 66(10), 3233-3244.

Mogensen, G. T., Espinosa, H. G., and Thiel, D. V., 2014. Surface impedance mapping using sferics: *Geoscience and Remote Sensing*, 52(4), 2074-2080.

Oliver, John E., 2008, *Encyclopedia of world climatology*: Springer Science & Business Media, p. 452

Thiel, D. V. and Mittra, R., 1997, An analysis of a staked dipole probe on a lossy earth plane using the finite-difference time-domain method, *Geoscience and Remote Sensing*, 35(5), 1357-1362.